

Numerical Analysis of Gas Diffusion Characteristics during Thermal Runaway in ESS Battery Module

Dong Woo Kim¹, Young Man Lee¹, Hong Sun Ryou²

¹Fire Prevention System Institution/Alllifelife Co., Ltd.

72 Deockcheon-ro 72, Manan-gu, Anayang-si 01847, Republic of Korea

First.dwkim@alllifelife.com; Second.ymlee@alllifelife.com

²School of Mechanical Engineering /Chung-Ang University

84 Heukseok-ro Dongjak-gu, Seoul 06974, Republic of Korea

Third.cfdmec@cau.ac.kr

Abstract - Energy storage system(ESS) is an eco-friendly energy storage system but it has safety problems due to explosions and toxic gas. Because the fire in the ESS system is caused by the thermal runaway of the battery, early detection would be essential to avoid fire damage. Gas composition and gas diffusion during thermal runaway are important factors for early detection. Most of this research has been conducted in the battery cells. However, the ESS system consists of battery modules. The spacing distance between battery cells and the module shape affects the gas diffusion for modules. Therefore, the present study aims to numerically examine the gas diffusion characteristics during thermal runaway inside the battery modules, and estimate the time required for detection. Simulations were performed for three cases depending on the fire locations. Numerical results showed that the CO₂ concentration in EES modules reached 5,000 ppm as the criterion for detection, within 20 seconds after a fire occurs. In addition, faster detection would be possible when the sensors are installed adjacent to the cells at which thermal runaway occurs.

Keywords: Energy storage system(ESS), Gas diffusion, Thermal runaway, CO₂, Detection

1. Introduction

Energy storage system(ESS) is a system that is storing energy and supplying power when necessary. ESS is a renewable, eco-friendly system, a technology receiving a lot of attention worldwide. Most of the energy storage used in this system uses lithium-ion batteries. Lithium-ion batteries have the advantages of high energy density, low memory effect, and low self-discharge. However, lithium-ion batteries have many unsafe factors, such as explosion and toxic gas emissions when occurs fire. Early detection of fire is one of the ways to prevent battery fires. From the point of view of early detection, gas composition and detection of temperature change in the event of a battery fire are important. The main cause of battery fires is thermal runaway. It is known that thermal runaway occurs when a battery is subjected to abuse conditions, and there are usually three conditions (mechanical, electrical, and thermal) [1]. The composition of released gas generated during a fire varies depending on the conditions of abuse, state of charge (SOC), and the battery components. However, most components of the emitted gas are H₂, CO₂, and CO [2]. Andrey W. Golubkov, Sebastian Scheikl, Rene Planteu, Gernot Voitic, Helmar Wilsche, Christoph Stangl, Gisela Fauler, Alexander Thaler and Viktor Hackerb.[3] investigated the gas component generated by triggering thermal runaway for each SOC of the 18,650 cylinder types NCA and LFP battery and confirmed that CO gas dominates when the battery is overcharged and CO₂ gas dominates when the battery is below 100%. Ting Cai, Puneet Valecha, Vivian Tran, Brian Engle, Anna Stefanopoulou, Jason Siegel.[4] investigated the toxic gas emission according to each abuse condition and battery electrode components through literature. They found that the CO₂ component is the most effective from the viewpoint of early detection. Qingsong Wang, Ping Pinga, Xuejuan Zhaoa, Guanquan Chub, Jinhua Suna, Chunhua Chenc.[5] tried to explain the decomposition process for each battery component when thermal runaway occurred and mentioned that CO₂ was released due to the decomposition of the internal electrolyte in the earliest stage of thermal runaway. For early detection of thermal runaway, Sascha Koch, Kai Peter Birke and Robert Kuhn.[6] conducted experiments to measure the time required for early detection with various sensors. They showed that the gas sensor most fastly detected thermal runaway, and the gas sensor detecting signal was strong compared to other sensors. However,

these previous studies have been conducted on battery unit cells. In the case of an ESS system, batteries are not stored in units of cells but in units of modules. There is a space inside the module, and the time for early detection of thermal runaway also varies depending on the install location of the sensor. Therefore, it is important to analyze the gas diffusion during the thermal runaway of the battery inside the module. Gas diffusion is affected by the shape of the module, the spacing between the battery cells, and the cell location where the thermal runaway was triggered. The present study carried out numerical simulations to examine gas diffusion characteristics and detection times for the various fire locations in the ESS battery module when thermal runaway occurs.

2. Numerical Simulations

2.1. Mathematical representations

The present study solves the conservation equations of mass, momentum with the species transport equation as follows: [7]

$$\frac{\partial \rho}{\partial t} = -\nabla \cdot (\rho \mathbf{u}) \quad (1)$$

The species transport equation is expressed as

$$\frac{\partial(\rho Y_i)}{\partial t} + \nabla \cdot (\rho \mathbf{u} Y_i) = -\nabla \cdot \mathbf{J}_i + R_i + S_i \quad (2)$$

where ρ represents the density, the \mathbf{u} is the velocity, R_i is the net rate of production of species i by chemical reaction, \mathbf{u} is the velocity and \mathbf{J}_i is the diffusion flux of species i , which arises due to concentration. Y_i means the local mass fraction of each species.

The standard $k - \epsilon$ model can be expressed as follows:

$$\frac{\partial(\rho k)}{\partial t} + \frac{\partial(\rho k u_i)}{\partial x_i} = \frac{\partial}{\partial x_j} \left[\left(\mu + \frac{\mu_t}{\sigma_k} \right) \frac{\partial k}{\partial x_j} \right] - \rho \epsilon \quad (3)$$

$$\frac{\partial(\rho \epsilon)}{\partial t} + \frac{\partial(\rho \epsilon u_i)}{\partial x_i} = \frac{\partial}{\partial x_j} \left[\left(\mu + \frac{\mu_t}{\sigma_\epsilon} \right) \frac{\partial \epsilon}{\partial x_j} \right] + C_{1\epsilon} \frac{\epsilon}{k} - C_{2\epsilon} \frac{\epsilon^2}{k} \quad (4)$$

$$\mu_t = C_\mu \frac{\rho k^2}{\epsilon} \quad (5)$$

where k represents the turbulent kinetic energy, μ represents the dynamic viscosity, μ_t represents eddy viscosity, ϵ represents the dissipation rate. We used the commercial program ANSYS Fluent (v. 18.0) to simulate gas diffusion behavior when the thermal runaway occurs. Figure 1 shows the computational domain with the attached and the battery cell specification. The number of cells in the module are 28.

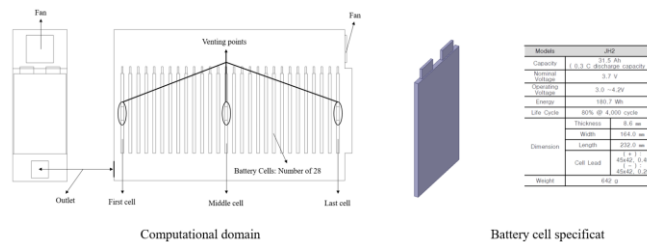


Fig. 1: The computation domain and battery cell specification

2.2. Boundary conditions and numerical details

Figure 2 shows the boundary conditions. The previous study showed that CO₂ emission was caused by electrolyte decomposition when a cell temperature reached 90 °C in the first step during thermal runaway. The same conditions were set in this study. The red circle in Figure 2 is the location where CO₂ gas is released during thermal runaway. CO₂ gas during thermal runaway is released from the side of battery cells. The module's fan is no longer operated after the occurs fire. Hence, the simulation does not consider the fan operation. The module outside is atmospheric pressure. The time step was 0.01 s and set to the analysis time 100 s. The species transport model was used for the gas release during thermal runaway. We used gas-released data from reference 4. The present study considered three cases where thermal runaway occurred in the first cell, middle cell, and last cell and used the standard $k - \epsilon$ model for turbulent flows. Figure 3 shows the grid system with hexahedral meshes and their number of approximately 3,000,000.

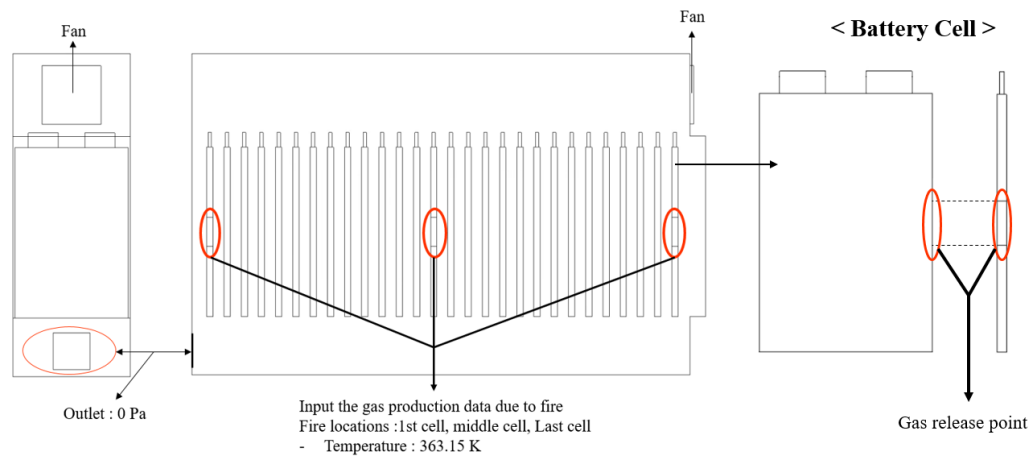


Fig. 2: The boundary conditions

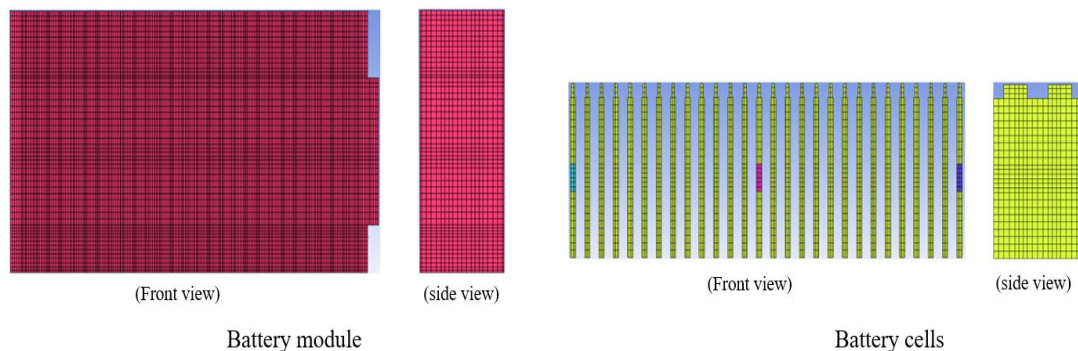


Fig. 3 The grid system for numerical analysis

3. Results and Discussions

Figure 4 shows the CO₂ mass fraction at the center plane of the module from 1 to 20 seconds. In the first cell case, CO₂ diffuses near the cell where the thermal runaway is triggered. CO₂ gas is initially diffused to the module top and bottom due to the adjacent module wall near the thermal runaway activated cell. After that, over time, the CO₂ diffuses completely into the module. For the middle cell, CO₂ gas diffuses over time around the cell in thermal runaway because there is no adjacent module wall. In the case of the last cell, there is an empty space near the cell where thermal runaway occurred. CO₂ gas diffuses into space near the cell where thermal runaway occurred. It then spreads inside the module.

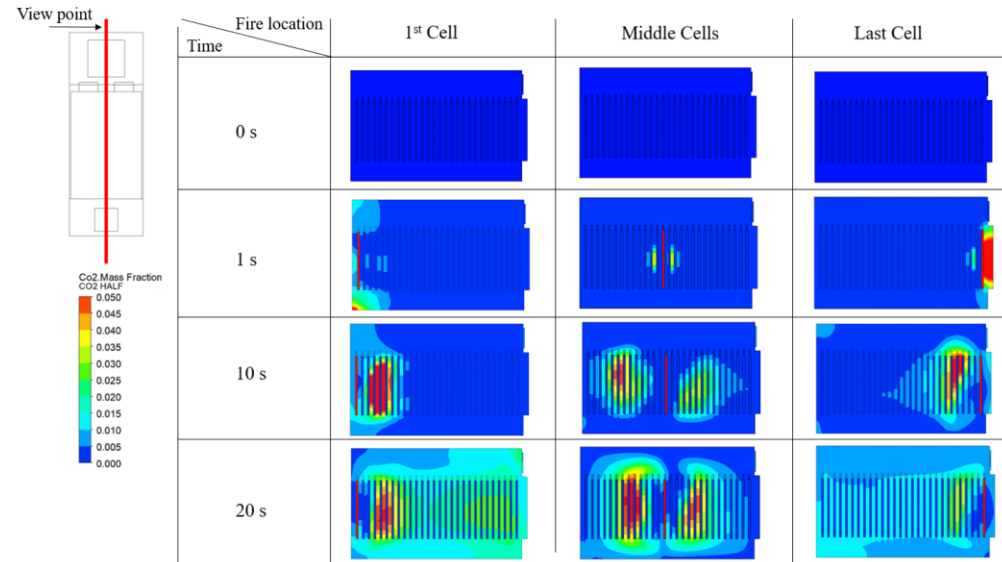


Fig. 4: CO₂ mass fraction at the center of the module from 1 to 20 seconds.

Figure 5 shows the CO₂ mass fraction at the center plane of the module from 40 to 80 seconds. In all cases, the difference in the CO₂ mass fraction after 60 seconds is insignificant.

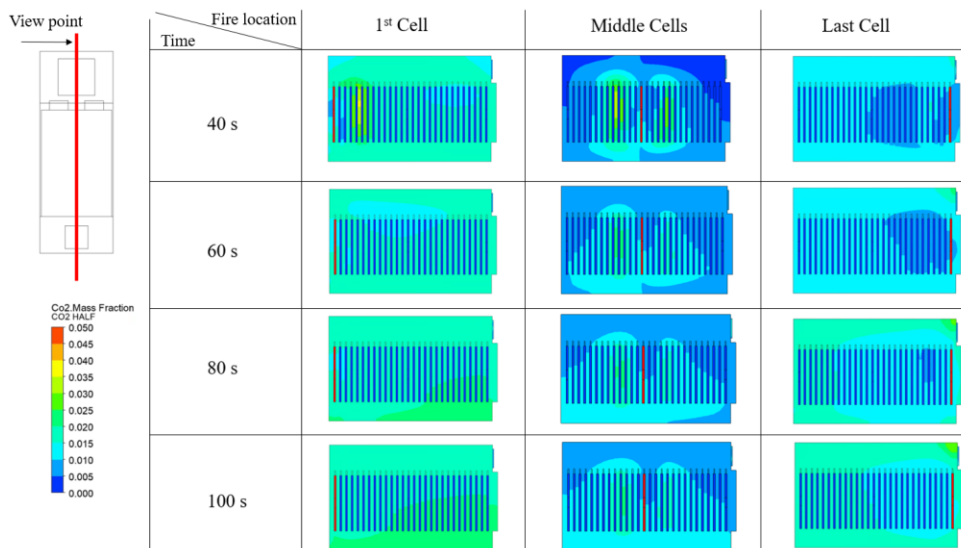


Fig. 5: CO₂ mass fraction at the center of the module from 40 to 80 seconds

Figure 6 depicts Gas velocity and CO₂ mass fraction along the fan line in the center plane of the module during thermal runaway in the first cell. Fan line is a line at the module center from the center of the fan to the module wall. When thermal runaway occurs in the first cell, velocity distribution and CO₂ mass fraction little differ after 40 seconds. This indicates that CO₂ is filled with inside the module. When gas is released due to thermal runaway in the first cell, the velocity distribution along the fan line is the fastest at 10 seconds. Initially, there is no gas inside the module, so the gas diffusion velocity is fast due to the concentration difference. Conversely, the CO₂ mass fraction is lowest at 10 seconds. In the adjacent cell where the thermal runaway occurred, the gas diffuses and the mass fraction of CO₂ is high,

and the mass fraction of CO_2 gradually decreases as it moves away from the cell where the thermal runaway occurred. Therefore, at 10 seconds, the gas released due to thermal runaway is in the process of being diffused into the module. There is a slight difference after 20 seconds in the velocity distribution, but the trend is similar. It can be confirmed that the gas due to thermal runaway spreads after 20 seconds along the fan line. It can be seen that the velocity distribution after 30 seconds fluctuates. It means that the gas from the fan line diffuses into the space between the cells. From a detection point of view, CO_2 sensors have different detection ranges for each sensor. In this study, it was assumed that the sensor can detect CO_2 when the CO_2 concentration is above 5,000 ppm. The red horizontal line in the CO_2 mass fraction graph is based on 5,000 ppm. In case of thermal runaway in the first cell, the released gas rapidly diffuses into the module at 10 seconds, but the amount of gas emitted is small. Therefore, if the CO_2 sensor is installed in a cell adjacent to a thermal runaway in the fan line, it can detect more than 5,000 ppm of CO_2 . In practice, it is impossible to predict where thermal runaway will occur, making it difficult to install sensors in adjacent cells where thermal runaway has occurred. After 20 seconds, the CO_2 sensor can be detected CO_2 in any area of the fan line. Therefore, it takes about 20 seconds to detect above 5,000 PPM of CO_2 .

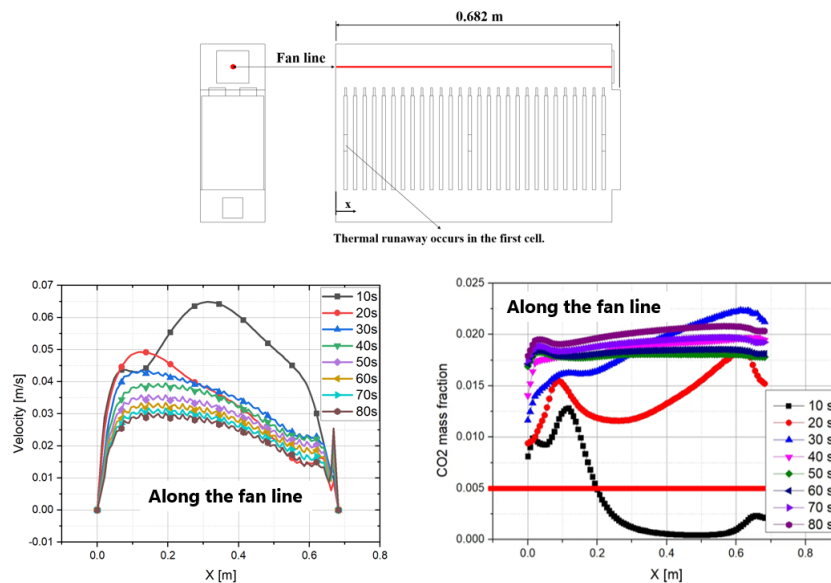


Fig. 6: Velocity distribution and CO_2 mass fraction along the fan line in the center plane of the module during thermal runaway in the first cell.

Figure 7 provides the estimated velocity distribution and CO_2 mass fraction along the outlet line in the center of the module during thermal runaway in the first cell. The diffusion process is similar to the fan line results. At 10 seconds, the velocity distribution along the outlet line spreads rapidly into the module because there is no gas released due to thermal runaway inside the module. As the gas diffuses inside the module according to time, the difference in concentration between the gas released by thermal runaway and the diffused gas inside the module is reduced. The gas diffusion velocity inside the module gradually slows down according to time. These results can be seen in the velocity distribution after 20 seconds. Additionally, it can be seen that the velocity distribution varies after 30 seconds, this means that gas due to thermal runaway along the outlet line diffuses into the region between the cells. After 40 seconds, the change in velocity distribution is insignificant. This means that the released gas due to thermal runaway fills up all the module. Unlike the result in the fan line, in the outlet line, the gas released during thermal runaway flows toward the outlet, so it cannot be detected by the CO_2 sensor within 10 seconds. After 20 seconds, More than 5,000 ppm of CO_2 can be detected in most areas of the outlet line. As in 10 seconds, it is difficult to detect CO_2 near the outlet due to the gas being emitted towards the outlet. Therefore, to detect

CO₂ when thermal runaway occurs in the first cell, it is efficient to install on the fan line because it can detect CO₂ above 5,000 ppm in any area of the fan line.

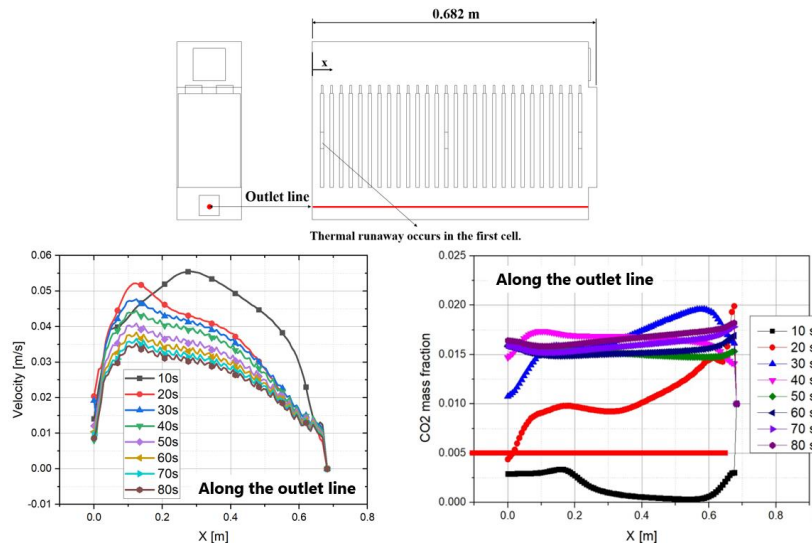


Fig. 7: velocity distribution and CO₂ mass fraction along the outlet line in the center of the module during thermal runaway in the first cell.

Figure 8 shows the velocity distribution and CO₂ mass fraction along the fan line and outlet line in the center of the module during thermal runaway in the last cell. When thermal runaway occurs in the last cell, the gas firstly diffuses into the space in front of the module and then spreads throughout the module. Therefore, for thermal runaway in the last cell, the velocity distribution along the fan line at 10 seconds is not much different from that of 20 seconds. At the outlet line, the velocity distribution at $x < 0.05$ is affected by outlet. After 20 seconds, the same diffusion process occurs as in the first cell. If a CO₂ sensor is installed the adjacent cell where thermal runaway occurs in the fan line and the outlet line, it is possible to detect CO₂ (above 5,000 ppm) within 10 seconds. After 20 seconds, it can detect more than 5,000 ppm of CO₂ in any region of the fan line and outlet line.

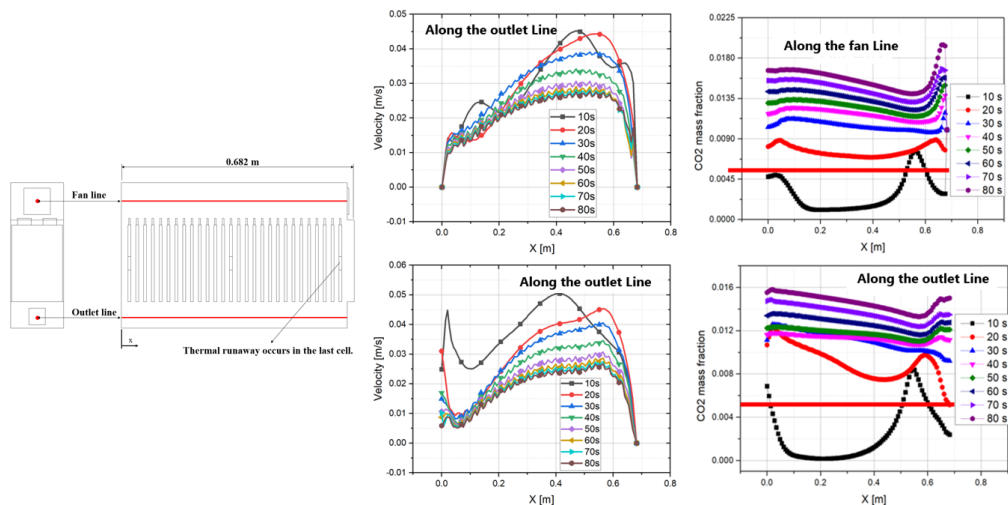


Fig. 8: Velocity distribution and CO₂ mass fraction along the fan line and outlet line in the center of the module during thermal runaway in the last cell.

Figure 9 show the velocity distribution and CO₂ mass fraction along the fan line and outlet line in the center of the module during thermal runaway in the middle cell. When thermal runaway occurs in the middle cell, there is no significant difference in the gas diffusion velocity distribution after 40 seconds. This indicates that the inside of the module is completely full of CO₂. Also, since gas diffusion proceeds from the center of the module to both sides of the module, gas diffusion is slower than when thermal runaway occurs in the first and last cells. It cannot be detected CO₂ above 5,000 ppm along the fan line and outlet line within 10 seconds. After 20 seconds, CO₂ sensor can be detected CO₂ above 5,000 ppm any region of the outlet line. However, there are areas in the fan line that cannot be detected CO₂ above 5,000 ppm at 20 seconds. Therefore, it is efficient to install at the outlet line because it can detect 5000 ppm concentration of CO₂ in any area along the outlet line.

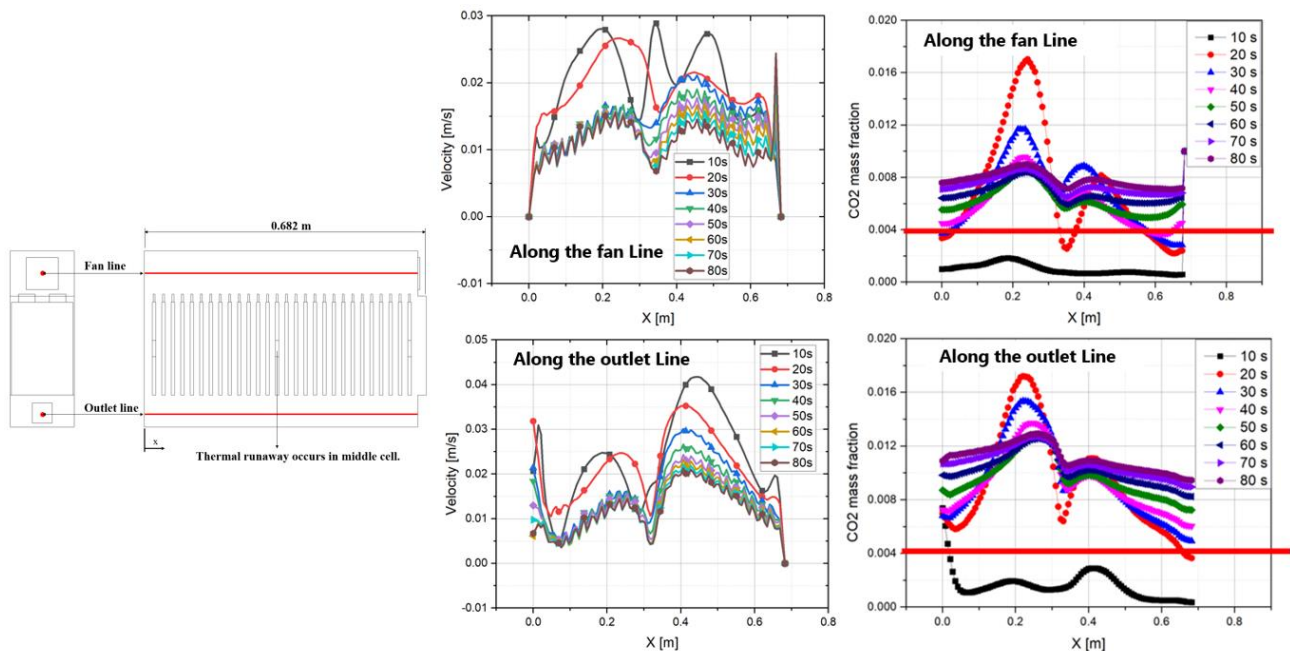


Fig. 9: Velocity distribution and CO₂ mass fraction along the fan line and outlet line in the center of the module during thermal runaway in the middle cell.

4. Conclusion

In this study, the diffusion of CO₂ gas during thermal runaway was analysed, and the time required to detect it and the appropriate sensor location was confirmed. Regardless of the cell location in the module, it takes about 40 seconds for CO₂ to fill the inside of the module during thermal runaway completely. If thermal runaway occurs in the first and last cells, it can be detected in less than 10 seconds, but it is impossible because the sensor must be located in the adjacent cell where the thermal runaway occurred. Therefore, it takes about 20 seconds to detect CO₂ above 5,000 ppm during thermal runaway, and CO₂ can be detected anywhere in the fan line and the outlet line. When thermal runaway occurs in the middle cell, it is impossible to detect CO₂ within 10 seconds, even though a sensor is installed adjacent to the thermal runaway in the cell. After 20 seconds, it is possible to detect 5000 ppm concentration of CO₂ along the fan line and the outlet line. However, there is a point where CO₂ is not detected CO₂ above 5,000 ppm in the fan line at 20 seconds. Therefore, it is advantageous to install a CO₂ sensor in the outlet line.

Acknowledgements

This work was supported by the Research and Development of Fire Safety Technology for ESS Hydrogen Facilities, 20011568.

References

- [1] Xuning Feng, Mingguo Ouyang, Xiang Liu, Languang Lu, Young Xia, and Xiangming He. “Thermal runaway mechanism of lithium ion battery for electric vehicles: a review.”, *Energy Storage Mater*, vol. 10, 246-267, 2018.
- [2] Andrey W. Golubkov, David Fuchs, Julian Wagner, Helmar Wiltsche, Christoph Stangl, Gisela Fauler, Gernot Voitic, Alexander Thaler and Viktor Hacker. “Thermal-runaway experiments on consumer li-ion batteries with metal-oxide and olivin-type cathodes”, *RSC Advances*, vol. 4, pp. 3615-3620, 2014
- [3] Andrey W. Golubkov, Sebastian Scheickl, Rene Planteu, Gernot Voitic, Helmar Wiltsche, Christoph Stangl, Gisela Fauler, Alexander Thaler and Viktor Hackerb “Thermal runaway of commercial 18650 li-ion batteries with LFP and NCA cathodes–impact of state of charge and overcharge”, *RSC Advances*, vol. 5, pp. 57171-57186, 2015
- [4] Ting Cai, Puneet Valecha, Vivian Tran, Brian Engle, Anna Stefanopoulou, Jason Siegel. “Detection of Li-ion battery failure and venting with carbon dioxide”, *eTransportation*, vol. 7, 100100, 2021
- [5] Qingsong Wang, Ping Pinga, Xuejuan Zhaoa, Guanquan Chub, Jinhua Suna, Chunhua Chenc. “Thermal runaway caused fire and explosion of lithium ion battery”, *Journal of Power Sources*, vol. 208, pp. 210-224, 2012
- [6] Sascha Koch, Kai Peter Birke and Robert Kuhn. “Fast thermal runaway detection for lithium-Ion cells in large scale traction batteries”, *Batteries*, vol. 4, Issue 2, 16, 2018
- [7] ANSYS FLUENT 18.0 theory guide. ANSYS Inc.; 2017